

# Training Artificial Neural Networks by Generalized Likelihood Ratio Method: Exploring Brain-like Learning to Improve Adversarial Defensiveness

Li Xiao<sup>a</sup>, Yijie Peng<sup>\*b</sup>, Jeff Hong<sup>c</sup>, and Zewu Ke<sup>a</sup>

<sup>a</sup>Institute of Computing Technology, Chinese Academy of Science, Beijing, China, Email: xiaoli@ict.ac.cn

<sup>b</sup>Peking University, Beijing, China, Email: pengyijie@pku.edu.cn

<sup>c</sup>Fudan University, Shanghai, China, Email: hong\_liu@fudan.edu.cn

## Abstract

Recent work in deep learning has shown that the artificial neural networks are vulnerable to adversarial attacks, where a very small perturbation of the inputs can drastically alter the classification result. In this work, we propose a generalized likelihood ratio method capable of training the artificial neural networks with some biological brain-like mechanisms, e.g., (a) learning by the loss value, (b) learning via neurons with discontinuous activation and loss functions. The traditional back propagation method cannot train the artificial neural networks with aforementioned brain-like learning mechanisms. Numerical results show that various artificial neural networks trained by the new method can significantly improve the defensiveness against the adversarial attacks. Code is available: [https://github.com/LX-doctorAI/GLR\\_ADV](https://github.com/LX-doctorAI/GLR_ADV).

on the loss between the ANN output and target data. The back propagation (BP) method has been the most widely used technique to iteratively train ANNs. However, the BP method requires the loss function and activation function to be smooth in ANN, which limits the capability of ANNs to fit well with the surrounding environments.

Recent work in deep learning has demonstrated that ANNs are vulnerable to adversarial attacks, where a very small perturbation of the inputs can drastically alter the classification result. The adversarial attacks could pose severe security threats to a wide range of critical deep learning systems (Cao & Gong, 2017; Carlini & Wagner, 2017; Carlini et al., 2016; Elsayed et al., 2018; Eykholt et al., 2018; Liao et al., 2017; N. Papernot & Swami, 2016; S. Sabour & Fleet, 2015). For instance, attackers could use adversarial samples to confuse the face-recognition or voice recognition system to compromise a financial or government entity (Cao & Gong, 2017); a self-driving vehicle may take unexpected actions and cause accidents if the vision camera misclassifies some important signals (Carlini et al., 2016).

Several approaches have been developed to address the problem by penalizing the adversarial directions in training. This requires to know the adversarial directions of ANNs a priori, which may not always be easy (Alhussein Fawzi & Frossard, 2016; Carlini & Wagner, 2017; Gu & Rigazio, 2014; Osbert Bastani & Criminisi, 2016; Seyed-Mohsen Moosavi-Dezfooli & Frossard, 2016). Moreover, the cause of the adversarial phenomena still remains unclear. The problem was originally thought due to extreme nonlinearity and insufficient regularization of the ANN (C. Szegedy & Fergus, 2014), but Goodfellow et al., 2014 showed that even linear models are sufficient to cause the adversarial phenomena. In addition, it has been discovered that the same adversarial samples can effectively attack a variety of ANNs under distinctive architectures and trained by different data sets, which makes the security issue on using ANNs more

## 1. Introduction

Artificial neural network (ANN) has been used as a universal classifier. In recent years, there have been tremendous successes in applying ANNs to image processing, speech recognition, game, and medical diagnosis (Esteva et al., 2017; Graves et al., 2013; Gulshan et al., 2016; He et al., 2016; Silver et al., 2016). In ANN, the inputs such as texts and images are turned into a vector, and each neuron performs a nonlinear transformation on the input vector. A deep learning ANN typically contains multiple layers of convoluted neurons. This complicated machinery maps the input space to the target space. There are synaptic weights in each neuron to be adapted to the surrounding environment based

\*Corresponding Author

of concerns in practice.

In contrast, the adversarial phenomenon rarely happens for human being (Elsayed et al., 2018). Then some interesting questions arise: what are the differences between biological neural networks in the human brains and ANNs? Can we borrow some mechanisms from the biological brain neural networks to improve the defensiveness of ANNs? There are some noticeable differences between the neurons in human brain and the neurons used in traditional ANNs (Dayan & Abbott, 2018). First, the activation of the brain neuron is via an electric impulse, which can be captured by a threshold activation function, and there exists a (neuronal) noise in each neuron, whereas the traditional ANN uses continuous activation functions, e.g., Sigmoid and ReLu, and a deterministic nonlinear transformation. Second, human brain perceives an object as a specific category, e.g., dog or cat, which means that the loss function capturing the mechanism of a human brain should be a discontinuous zero-one function, whereas the loss functions in ANNs are smooth, e.g., the cross-entropy function. Furthermore, the brain neuron network is effected directly by the electronic signal sent by a sensory system and the chemical signal from the endocrine, therefore the biological brain functions like learning from the loss value itself rather than the gradient of the loss, which the BP method uses.

In this work, a generalized likelihood ratio (GLR) method is proposed to train ANNs with neuronal noises. Unlike the BP method, GLR trains ANNs directly by the loss value, rather than the gradient of the loss. Since GLR does not differentiate the sample path of the loss, it can train ANNs with discontinuous activation and loss functions. Therefore, the new training method generalizes the scope of ANNs to be used in practice, which allows some brain-like mechanisms, i.e., (a) learning by the loss value and (b) learning via neurons with discontinuous activation functions and neuronal noises. The complexity in calculating the GLR estimator is also simpler than the BP method, because there is no need to calculate the backward propagation for the derivatives of the error signals.

The GLR method is a recent advance in stochastic gradient estimation studied actively in the area of simulation optimization (Asmussen & Glynn, 2007, Fu, 2015, Peng et al., 2018). Infinitesimal perturbation analysis (IPA) and the likelihood ratio (LR) method are two classic unbiased stochastic gradient estimation techniques (Ho & Cao, 1991, Glasserman, 1991, Hong, 2009, Rubinstein & Shapiro, 1993, Pflug, 1996, Heidergott & Leahu, 2010). IPA allows the parameters in the performance function but requires the continuity (differentiability) of the performance function; LR does not allow the parameters in the performance function, whereas it does not require continuity of the performance function. The GLR method extends two classic methods to a setting

allowing both the parameters in the performance function and discontinuous performance function, so that it can be applied to train the parameters in discontinuous ANNs.

We test the classification performances of various ANNs under the attacks of the adversarial samples. All the ANNs have the same number of layers and neurons but different activation and loss functions. The defensiveness against the adversarial attacks of all ANNs trained by the GLR method is significantly improved compared with an ANN with the Sigmoid activation function and cross-entropy loss function trained by the BP method. Incorporating the discontinuous activation and loss functions into ANNs trained by GLR also appears to have the potential on further enhancing defensiveness against the adversarial attacks under some circumstances.

## 2. Method

### 2.1. Setup and Background

Suppose we have inputs  $\vec{X}^{(1)}(n) := (x_1^{(1)}(n), \dots, x_{m_1}^{(1)}(n))$ ,  $n = 1, \dots, N$ . For the  $n$ th input, the  $i$ th output of the  $t$ th level of neurons is given by

$$v_i^{(t)}(n) := \sum_{j=0}^{m_t} \theta_{i,j}^{(t)} x_j^{(t)}(n) + r_i^{(t)}(n),$$

$$x_i^{(t+1)}(n) := \varphi(v_i^{(t)}(n)), \quad i = 1, \dots, m_{t+1},$$

where  $x_j^{(t)}(n)$  is the  $j$ th input of the  $t$ th level of neurons ( $j$ th output of the  $(t-1)$ th level of neurons),  $\theta_{i,j}^{(t)}$  is a synaptic weight,  $r_i^{(t)}(n)$  is a noise with density function  $f_{i,t}(r_i^{(t)}(n))$ ,  $v_i^{(t)}(n)$  is the  $i$ th signal, and  $\varphi$  is the activation function. The synaptic weights  $\theta_{i,j}^{(t)}$ ,  $j = 0, \dots, m_t$ , are the parameters to be trained in the ANN. It is required that  $x_0^{(t)}(n) \equiv 1$ , and  $\theta_{i,0}^{(t)}$  is called a bias. Figure 1 illustrates the structure of a neuron in the ANN.

The classic ANN does not include the noise, i.e.,  $r_i^{(t)}(n) \equiv 0$ , and the ANN considered in our work generalizes the classic one by adding a (random) noise to the neurons. The activation function  $\varphi$  is a nonlinear function. The Sigmoid function is a popular activation function defined by

$$\varphi_s(v) := 1/(1 + \exp(-sv)),$$

where  $s > 0$  is a constant. The Sigmoid function is smooth. Notice that with parameter  $s$  increasing to infinity, the Sigmoid function converges to a threshold function, i.e.,

$$\lim_{s \rightarrow \infty} \varphi_s(v) = \varphi_o(v) := \begin{cases} 1 & \text{if } v > 0, \\ 0 & \text{if } v < 0. \end{cases}$$

In Figure 2, we can see the curves of the Sigmoid functions with different parameters and the threshold function.

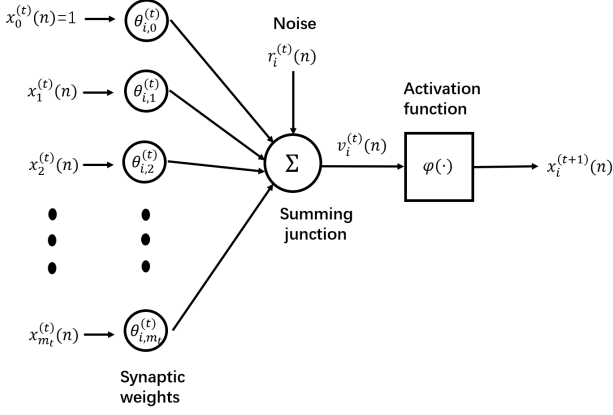


Figure 1. Structure of a neuron.

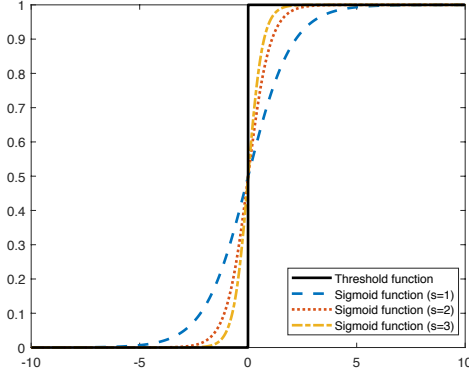


Figure 2. Threshold and Sigmoid activation functions.

Suppose the ANN has  $\tau$  levels of neurons, and  $\vec{X}^{(\tau)}(n) := (x_1^{(\tau)}(n), \dots, x_{m_\tau}^{(\tau)}(n))$  is the output vector of the ANN given the  $n$ th input data. Let  $\vec{O}(n) := (o_1(n), \dots, o_{m_\tau}(n))$  be the real observation vector given the  $n$ th input data, and  $L(\vec{X}^{(\tau)}(n), \vec{O}(n))$  be a loss function of the outputs of ANN and observations. In classification, a popular loss function is the cross-entropy loss function given by

$$L_c(\vec{X}^{(\tau)}(n), \vec{O}(n)) = - \sum_{i=1}^{m_\tau} o_i(n) \log \left( p_i(\vec{X}^{(\tau)}(n)) \right),$$

where

$$p_i(\vec{X}^{(\tau)}(n)) := \frac{\exp \left( x_i^{(\tau)}(n) \right)}{\sum_{j=1}^{m_\tau} \exp \left( x_j^{(\tau)}(n) \right)}, \quad i = 1, \dots, m_\tau.$$

The functions  $p_i$ ,  $i = 1, \dots, m_\tau$ , are called softmax functions. Note that the cross-entropy loss function is smooth. Alternatively, we can also use the following 0-1 loss func-

tion:

$$L_o(\vec{X}^{(\tau)}(n), \vec{O}(n)) = \mathbf{1} \left\{ \max_{i=1, \dots, m_\tau} p_i(\vec{X}^{(\tau)}(n)) = \max_{i=1, \dots, m_\tau} o_i(\vec{X}^{(\tau)}(n)) \right\}.$$

To train the ANN, we want to minimize the expected loss:

$$\mathcal{E}(\theta) = \mathbb{E} \left[ L(\vec{X}^{(\tau)}(n), \vec{O}(n)) \right]$$

where  $\theta$  is a vector containing all synaptic weights. To solve the optimization, the stochastic approximation (SA) (Kushner & Yin, 2003) is applied

$$\theta(n) = \theta(n-1) - \lambda_n G(n), \quad (1)$$

where  $\lambda_n$  is the learning rate and  $G(n)$  is an unbiased stochastic gradient estimator of  $\mathcal{E}(\theta)$ , i.e.,

$$\mathbb{E}[G(n)] = \nabla_{\theta} \mathcal{E}(\theta) |_{\theta=\theta(n-1)}. \quad (2)$$

The BP method is the most popular stochastic gradient estimator (Haykin, 2009):

$$B_{a,b}^{(l)}(n) := \delta_a^{(l+1)}(n) x_b^{(l)}(n),$$

where  $B_{a,b}^{(l)}(n)$  is an unbiased stochastic derivative estimator with respect to synaptic weight  $\theta_{a,b}^{(l)}$ , and

$$\delta_i^{(t)}(n) := \begin{cases} e_i^{(\tau)}(n) \varphi' \left( v_i^{(\tau-1)}(n) \right), & \text{if } t = \tau, \\ \varphi' \left( v_i^{(t-1)}(n) \right) \left( \sum_{j=1}^{m_t} \theta_{j,i}^{(t)} \delta_j^{(t+1)}(n) \right), & \text{if } t < \tau, \end{cases} \quad (3)$$

with the error signal  $e_i^{(\tau)}(n)$  defined by

$$e_i^{(\tau)}(n) := \frac{\partial L(\vec{X}^{(\tau)}(n), \vec{O}(n))}{\partial x_i^{(\tau)}(n)}.$$

## 2.2. Generalized Likelihood Ratio method

Peng et al., 2019 prove that the BP algorithm is mathematically equivalent to IPA, but the computational complexity of BP is lower. BP directly differentiates the sample path of the output, so it requires the sample path of the output is Lipschitz continuous and differentiable almost surely. Therefore, BP cannot deal with the stochastic gradient estimation for ANN with discontinuous activation function and loss function. ANN used in our work may contain a discontinuous activation or loss function, which leads to a discontinuous sample path of the output. A push-out LR method proposed in Peng et al., 2019 can deal with the stochastic gradient estimation for ANN with discontinuous activation function and loss function. Here we derive a GLR estimator which coincides with the push-out LR estimator

for the first-order gradient in Peng et al., 2019 under a special case with the Sigmoid activation and a bounded loss function with a bounded gradient. The derivation shows the connection between the GLR method and the BP method. We construct an ANN with the Sigmoid activation function:

$$u_i^{(t)}(n) := \sum_{j=0}^{m_t} \theta_{i,j}^{(t)} y_j^{(t)}(n) + r_i^{(t)}(n)$$

$$y_i^{(t+1)}(n) := \varphi_s \left( u_i^{(t)}(n) \right), \quad i = 1, \dots, m_{t+1},$$

and an ANN with the threshold activation function:

$$\eta_i^{(t)}(n) := \sum_{j=0}^{m_t} \theta_{i,j}^{(t)} z_j^{(t)}(n) + r_i^{(t)}(n)$$

$$z_i^{(t+1)}(n) := \varphi_o \left( \eta_i^{(t)}(n) \right), \quad i = 1, \dots, m_{t+1}.$$

**Theorem 1.** Assuming that density function  $f_{a,l}(\cdot)$  of the noise  $r_a^l(n)$  (added to the  $a$ -th output of the  $(l-1)$ -th level of neurons) is differentiable and loss function  $L(\cdot)$  is bounded and with a bounded gradient w.r.t.  $\vec{X}^{(\tau)}(n)$ , we have

$$\frac{\partial}{\partial \theta_{a,b}^{(l)}} \mathbb{E} \left[ L(\vec{Z}(n), \vec{O}(n)) \right]$$

$$= \mathbb{E} \left[ -L(\vec{Z}(n), \vec{O}(n)) z_b^{(l)}(n) \frac{\partial \log f_{a,l}(r_a^{(l)}(n))}{\partial r_a^{(l)}(n)} \right].$$

*Proof.* We have

$$\frac{\partial L(\vec{Y}^{(\tau)}(n), \vec{O}(n))}{\partial \theta_{a,b}^{(l)}} = \sum_{i=1}^{m_\tau} \frac{\partial L(\vec{Y}^{(\tau)}(n), \vec{O}(n))}{\partial y_i^{(\tau)}(n)} \frac{\partial y_i^{(\tau)}(n)}{\partial \theta_{a,b}^{(l)}},$$

where  $\vec{Y}^{(\tau)}(n) := (y_1^{(\tau)}(n), \dots, y_{m_\tau}^{(\tau)}(n))$ , and

$$\frac{\partial y_i^{(t+1)}(n)}{\partial \theta_{a,b}^{(l)}} = \varphi'_s \left( u_i^{(t)}(n) \right) \frac{\partial u_i^{(t)}(n)}{\partial \theta_{a,b}^{(l)}},$$

$$\frac{\partial u_i^{(t)}(n)}{\partial \theta_{a,b}^{(l)}} = \sum_{j=0}^{m_t} \left( \frac{\partial \theta_{i,j}^{(t)}}{\partial \theta_{a,b}^{(l)}} y_j^{(t)}(n) + \theta_{i,j}^{(t)} \frac{\partial y_j^{(t)}(n)}{\partial \theta_{a,b}^{(l)}} \right).$$

In addition, we have

$$\frac{\partial L(\vec{Y}^{(\tau)}(n), \vec{O}(n))}{\partial \theta_{a,b}^{(l)}} = \sum_{i=1}^{m_\tau} \frac{\partial L(\vec{Y}^{(\tau)}(n), \vec{O}(n))}{\partial y_i^{(\tau)}(n)} \frac{\partial y_i^{(\tau)}(n)}{\partial z_a^{(l)}(n)},$$

where

$$\frac{\partial y_i^{(t+1)}(n)}{\partial r_a^{(l)}} = \varphi'_s \left( u_i^{(t)}(n) \right) \frac{\partial u_i^{(t)}(n)}{\partial r_a^{(l)}},$$

$$\frac{\partial u_i^{(t)}(n)}{\partial r_a^{(l)}} = \sum_{j=0}^{m_t} \left( \theta_{i,j}^{(t)} \frac{\partial y_j^{(t)}(n)}{\partial r_a^{(l)}} + \frac{\partial r_i^{(t)}(n)}{\partial r_a^{(l)}} \right).$$

Notice that

$$\frac{\partial u_a^{(l)}(n)}{\partial \theta_{a,b}^{(l)}} = y_b^{(l)}(n), \quad \frac{\partial u_a^{(l)}(n)}{\partial r_a^{(l)}} = 1.$$

It is straightforward to show

$$\frac{\partial L(\vec{Y}^{(\tau)}(n), \vec{O}(n))}{\partial \theta_{a,b}^{(l)}} \Big/ \frac{\partial L(\vec{Y}^{(\tau)}(n), \vec{O}(n))}{\partial r_a^{(l)}} = y_b^{(l)}(n).$$

Then,

$$\frac{\partial \mathbb{E} \left[ L(\vec{Y}^{(\tau)}(n), \vec{O}(n)) \right]}{\partial \theta_{a,b}^{(l)}} = \mathbb{E} \left[ \frac{\partial L(\vec{Y}^{(\tau)}(n), \vec{O}(n))}{\partial \theta_{a,b}^{(l)}} \right]$$

$$= \int_{\mathbb{R}} \frac{\partial L(\vec{Y}^{(\tau)}(n), \vec{O}(n))}{\partial \theta_{a,b}^{(l)}} f_{i,l}(r_a^{(l)}) dr_a^{(l)}$$

$$= \int_{\mathbb{R}} \frac{\partial L(\vec{Y}^{(\tau)}(n), \vec{O}(n))}{\partial r_a^{(l)}} \times \left( \frac{\partial L(\vec{Y}^{(\tau)}(n), \vec{O}(n))}{\partial \theta_{a,b}^{(l)}} \Big/ \frac{\partial L(\vec{Y}^{(\tau)}(n), \vec{O}(n))}{\partial r_a^{(l)}} \right) f_{i,l}(r_a^{(l)}) dr_a^{(l)}$$

$$= \int_{\mathbb{R}} x_b^{(l)}(n) \frac{\partial L(\vec{Y}^{(\tau)}(n), \vec{O}(n))}{\partial r_a^{(l)}} f_{i,l}(r_a^{(l)}) dr_a^{(l)}.$$

The interchange of derivative and expectation in the first equality can be justified by the dominated convergence theorem by noticing that the gradient of loss function  $L(\cdot)$  w.r.t.  $\vec{Y}^{(\tau)}(n)$  and the gradient of  $\vec{Y}^{(\tau)}(n)$  w.r.t.  $\theta_{a,b}^{(l)}$  are bounded. By integration by parts,

$$\int_{\mathbb{R}} y_b^{(l)}(n) \frac{\partial L(\vec{Y}^{(\tau)}(n), \vec{O}(n))}{\partial r_a^{(l)}} f_{i,l}(r_a^{(l)}) dr_a^{(l)}$$

$$= y_b^{(l)}(n) L(\vec{Y}^{(\tau)}(n), \vec{O}(n)) f_{i,l}(r_a^{(l)}) \Big|_{r_a^{(l)}=-\infty}^{\infty}$$

$$- \int_{\mathbb{R}} y_b^{(l)}(n) L(\vec{Y}^{(\tau)}(n), \vec{O}(n)) \frac{\partial f_{i,l}(r_a^{(l)})}{\partial r_a^{(l)}} dr_a^{(l)}$$

$$= \mathbb{E} \left[ -L(\vec{Y}^{(\tau)}(n), \vec{O}(n)) y_b^{(l)}(n) \frac{\partial \log f_{i,l}(r_a^{(l)})}{\partial r_a^{(l)}} \right],$$

where the first term is zero on the right hand side of the first equality because the loss function  $L(\cdot)$  and  $y_b^{(l)}(n)$  are bounded. By taking limit,

$$\lim_{s \rightarrow \infty} \mathbb{E} \left[ -L(\vec{Y}^{(\tau)}(n), \vec{O}(n)) y_b^{(l)}(n) \frac{\partial \log f_{i,l}(r_a^{(l)})}{\partial r_a^{(l)}} \right]$$

$$= \mathbb{E} \left[ \lim_{s \rightarrow \infty} -L(\vec{Y}^{(\tau)}(n), \vec{O}(n)) y_b^{(l)}(n) \frac{\partial \log f_{i,l}(r_a^{(l)})}{\partial r_a^{(l)}} \right]$$

$$= \mathbb{E} \left[ -L(\vec{Z}^{(\tau)}(n), \vec{O}(n)) x_b^{(l)}(n) \frac{\partial \log f_{i,l}(r_a^{(l)})}{\partial r_a^{(l)}} \right],$$

where  $\vec{Z}^{(\tau)}(n) := (z_1^{(\tau)}(n), \dots, z_{m_\tau}^{(\tau)}(n))$  and the interchange of limit and expectation in the first equality can be justified by the dominated convergence theorem by noticing that loss function  $L(\cdot)$  is bounded and  $y_b^{(l)}(n)$  is uniformly bounded in  $s$ . Moreover, for  $t < l$ ,

$$\lim_{s \rightarrow \infty} y_i^{(t)}(n) = z_i^{(t)}(n), \quad i = 1, \dots, m_t,$$

for bounded neighborhood  $\Theta_{a,b}^{(l)}$  containing  $\theta_{a,b}^{(l)}$ ,

$$\lim_{s \rightarrow \infty} \sup_{\theta_{a,b}^{(l)} \in \Theta_{a,b}^{(l)}} \left| y_b^{(l)}(n) - z_b^{(l)}(n) \right| = 0,$$

and

$$\lim_{s \rightarrow \infty} \sup_{\theta_{a,b}^{(l)} \in \Theta_{a,b}^{(l)}} \left| L(\vec{Y}^{(\tau)}(n), \vec{O}(n)) - L(\vec{Z}^{(\tau)}(n), \vec{O}(n)) \right| = 0,$$

which further leads to

$$\begin{aligned} & \lim_{s \rightarrow \infty} \sup_{\theta_{a,b}^{(l)} \in \Theta_{a,b}^{(l)}} \left| \mathbb{E} \left[ \left( L(\vec{Y}^{(\tau)}(n), \vec{O}(n)) y_b^{(l)}(n) \right. \right. \right. \\ & \left. \left. \left. - L(\vec{Z}^{(\tau)}(n), \vec{O}(n)) z_b^{(l)}(n) \right) \frac{\partial \log f_{i,l}(r_a^{(l)})}{\partial r_a^{(l)}} \right] \right| = 0. \end{aligned} \quad (4)$$

Summarizing the results above,

$$\begin{aligned} & \frac{\partial \mathbb{E} \left[ L(\vec{Z}^{(\tau)}(n), \vec{O}(n)) \right]}{\partial \theta_{a,b}^{(l)}} = \frac{\partial}{\partial \theta_{a,b}^{(l)}} \lim_{s \rightarrow \infty} \mathbb{E} \left[ L(\vec{Y}^{(\tau)}(n), \vec{O}(n)) \right] \\ & = \lim_{s \rightarrow \infty} \frac{\partial}{\partial \theta_{a,b}^{(l)}} \mathbb{E} \left[ L(\vec{Y}^{(\tau)}(n), \vec{O}(n)) \right] \\ & = \lim_{s \rightarrow \infty} \mathbb{E} \left[ -L(\vec{Y}^{(\tau)}(n), \vec{O}(n)) y_b^{(l)}(n) \frac{\partial \log f_{i,l}(r_a^{(l)})}{\partial r_a^{(l)}} \right], \end{aligned}$$

where the interchange of limit and derivative in the second equality is justified by uniform convergence (Eq.4). This proves the theorem.  $\square$

**Remark 1.** *Peng et al., 2019* show that for an ANN with certain smoothness in activation and loss functions,

$$B_{a,b}^{(l)}(n) = \frac{\partial L(\vec{X}^{(\tau)}(n), \vec{O}(n))}{\partial \theta_{a,b}^{(l)}}.$$

The GLR estimator is defined by

$$L_{a,b}^{(l)}(n) := L(\vec{X}(n), \vec{O}(n)) \omega_{a,b}^{(l)}(n), \quad (5)$$

where

$$\omega_{a,b}^{(l)}(n) := -x_b^{(l)}(n) \frac{\partial \log f_{a,l}(r_a^{(l)}(n))}{\partial r_a^{(l)}(n)}.$$

From the proof of Theorem 1, we can see that for an ANN under certain regularity conditions, the estimator of the

BP algorithm and the GLR estimator can be linked via integration by parts. For an ANN with a threshold activation function, the GLR estimator is derived by first smoothing the threshold activation function, which becomes the Sigmoid function, then integration by parts, and last taking limit to retrieve the threshold activation in the derivative estimator. These three components have also been used to derive the GLR method in a general framework (Peng et al., 2018), where we can find the smoothing technique is applied to a general discontinuous sample performance function without actually explicitly constructing the smoothing function. The GLR method can be generalized to deal with stochastic gradient estimation or even higher order gradient for the ANN with more general discontinuous activation and loss functions, which can be found in Peng et al., 2019.

**Remark 2.** In Eq.3, the BP method differentiates the loss and transmits the error signal from the output level backward throughout the entire ANN via the chain rule of the derivative, whereas in Eq.5, the GLR method does not differentiate the loss and directly uses the loss function scaled by a weight function, which can be viewed as an interaction between the interior mechanism of ANN and the loss in a surrounding environment, to train the ANN.

**Remark 3.** The BP method is computationally efficient because it only requires simulating a forward function propagation and backward error propagation for once, and the derivatives w.r.t. all synaptic weights  $\theta_{i,j}^{(t)}$ ,  $j = 1, \dots, m_t$ ,  $i = 1, \dots, m_{t+1}$ ,  $t = 1, \dots, \tau - 1$ , are estimated. The GLR method is even faster than BP, since its computation only contains one forward function propagation for estimating the derivatives w.r.t. all parameters. For a Gaussian random noise  $r_i^{(t)}$  with zero mean and variance  $\sigma_{i,t}^2$ , we have

$$\frac{\partial \log f_{i,t}(r_i^{(t)})}{\partial r_i^{(t)}} = -\frac{r_i^{(t)}}{\sigma_{i,t}^2}.$$

### 2.3. Implementation Details

In implementation, we add a Gaussian noise with zero mean and certain variance to each neuron. Then, the GLR gradient estimator used in Eq.5 for a synaptic weight associated with the signal from neuron  $b$  at the  $l$ -th level to neuron  $a$  at the  $(l+1)$ -th level is

$$\frac{L(\vec{X}(n), \vec{O}(n)) x_b^{(l)}(n) r_a^{(l)}}{\sigma_{a,l}^2}. \quad (6)$$

Here  $x_b^{(l)}$  is the signal from neuron  $b$  at the  $l$ -th level and  $r_a^{(l)}$  is the noise of neuron  $a$  at the  $(l+1)$ -th level,  $L(\vec{X}(n), \vec{O}(n))$  is the loss. For simplicity, we choose a common variance  $\sigma$  for the noises in all neurons. The training procedure by the GLR method is summarized in **Algorithm 1**.

---

**Algorithm 1** Training procedure by GLR

---

**Setup:** Input  $\vec{X}^{(1)}(n)$ , observations  $\vec{O}(n)$ , and variance  $\sigma$ .

**Step One:** Calculate loss output  $L(\vec{X}(n), \vec{O}(n))$  and the GLR gradient  $G(n)$  in Eq.2 via Eq.6.

**Iterations:** Replicate the above procedure  $K$  times to generate i.i.d. gradient estimates  $G_1(n), G_2(n), \dots, G_K(n)$ .

**Output:** An average of GLR gradient estimates  $\frac{1}{K} \sum_{i=1}^K G_i(n)$ , which is used in Eq.1 for updating parameter.

---

### 3. Experiments

#### 3.1. Dataset Preparation and Network Structure

We test the performance of the GLR method for training ANNs in the example of identifying the numbers from 0-9 of the MNIST dataset, where there are 10000 images in total. The images are split into the training set and testing set in a 6:4 ratio. Each image is resized to be a  $14 \times 14$ -pixels vector for facilitating the training. The appearance of the images is shown in Figure.3.



Figure 3. Images of the numbers in the MNIST dataset.

The ANN to be trained in the experiments have three layers: an input layer, a hidden layer, and an output layer. The structure of the ANN is depicted in Figure.4(a). The dimension of the input layer is 196, the same as the size of the image. The hidden layer has 20 neurons, and the output layer has 10 neurons representing 10 numbers. The integer value of the label needs to be converted into a 10-unit array as the target of the ANN. For example, when the label is 2, the target vector should be  $[0, 1, 0, 0, 0, 0, 0, 0, 0, 0]$ . The operations between the layers are illustrated in Figure.1. The inputs of the input layer and hidden layer first go through linear operations with Gaussian noises added on and then nonlinear activation functions are operated. The bias term in our ANN is set to be 1 at the head of each input array.

#### 3.2. Training Procedure

The number of replications in *Algorithm 1* is set as  $K = 10000$ . We apply the SA in Eq.1 with mini-batches and the batch size is set as 25, which takes about 12 seconds to run in python in a desktop with Intel i7-6700 CPU @ 3.40 GHz for each iteration. Each epoch contains 1680 iterations which takes about five hours to run. The step size is set as 0.1 and the noise variance is set as  $\sigma = 2$ . Peng et al., 2019 present many training results of the GLR method on classifying the handwritten data included in the python *sklearn* package. In Figure.5, we show the training and validation errors of

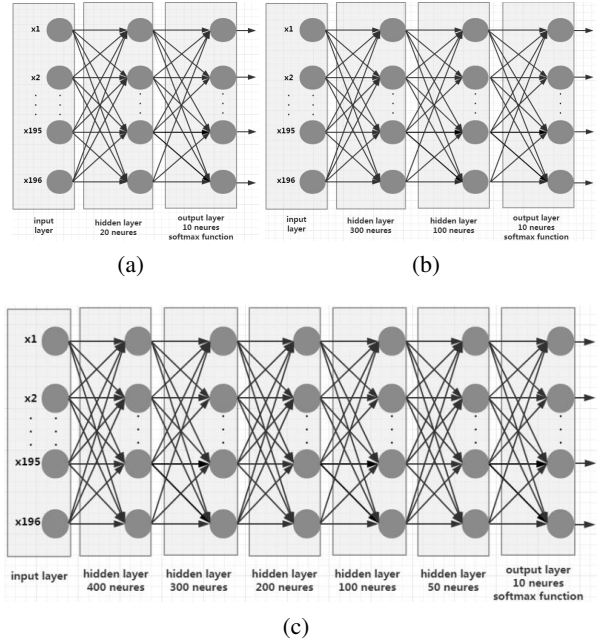


Figure 4. (a) Structure of ANN trained by the GLR method; (b), (c) Structure of ANN for generating adversarial samples with two hidden layers in (b) and five hidden layers in (c).

ANNs with the Sigmoid and threshold activation functions (as plotted in Figure.2) in the MNIST dataset, and the errors of ANNs converge fast after 12 epochs ( $\approx 20000$  iterations).

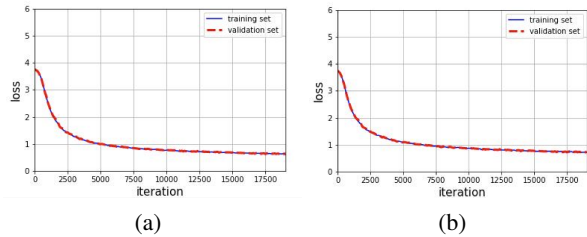


Figure 5. Losses in the training and validation sets of a single hidden layer ANN trained by GLR with activation functions as Sigmoid in (a) and threshold in (b), respectively.

#### 3.3. Adversarial Setting

We generate the adversarial samples using two different ANN structures. One ANN contains two hidden layers and one contains five hidden layers, which are depicted in (b) and (c) of Figure.4, respectively. The ANNs are trained and validated by the BP method, and then the fast gradient sign method (FGSM) (Goodfellow et al., 2014) is used to generate the adversarial samples of 5000 images randomly chosen from the testing set. The adversarial samples of the images are shown in Figure.6.

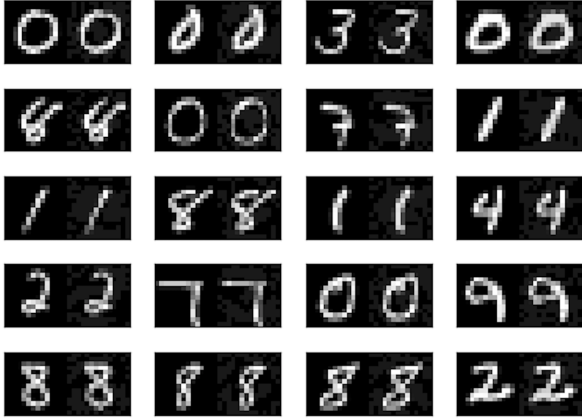


Figure 6. Samples of the paired images of the original samples (left) and adversarial samples (right). The adversarial samples are generated by ANN with two hidden layers in (b) of Figure.4.

### 3.4. Adversarial Testing

Adversarial testing is performed on several single hidden layers ANNs in Figure.4(a), with different activation and loss functions. For each adversarial sample, the predicted result is obtained from one of the following two criteria:

**1. One time (OT):** Run the classic ANN (without noise) using the parameters obtained from training and choose the category with the largest probability.

**2. Largest Average Probabilities (LAP):** Run the trained ANN with noises  $K = 10000$  times, compute the average probabilities of the 10 categories in 0-9, and choose the one with the largest average probability.

The accuracy is measured by the percentage of correct predictions over all the adversarial samples. The ANN with the same structure in (a) of Figure.4 trained by BP is used as the baseline for comparisons. Table.1 presents the results when adversarial samples are generated by the ANN with two hidden layers (Figure.4(b)); Table.2 presents the results when adversarial samples are generated by the ANN with five hidden layers (Figure.4(c)). The accuracies of the prediction on the original samples and the adversarial samples based on the above two criteria are presented.

Besides the Sigmoid and threshold activation functions, three other discontinuous activation functions shown in Figure.7 are also used in the experiments. Each test runs for 12 epochs and all of them demonstrate high accuracies on predicting the original samples after training. We also test the performance of an ANN with 0-1 loss function (the loss is 0 for a correct prediction and 1 otherwise), trained by the GLR. The ANN with 0-1 loss converges much slower than the classic cross entropy loss (See Table.1 and 2), so we run 24 epochs in training.

Activations + Entropy	Acc_Orig	Acc_OT	Acc_LAP
Sigmoid (trained by BP)	0.99	0.28	
Sigmoid	0.98	0.45	0.45
Threshold	0.95	0.52	0.53
$y =  x $	0.96	0.53	0.53
$y = \arctan(1/x)$	0.98	0.45	0.45
$y = \ln -x $	0.97	0.41	0.42
Activations + 0-1 loss	Acc_Orig	Acc_OT	Acc_LAP
Sigmoid	0.87	0.58	0.59
Threshold	0.86	0.56	0.58
$y = \ln -x $	0.88	0.51	0.53

Table 1. Adversarial tests for ANNs with different activation and loss functions trained by GLR. The adversarial samples are generated by an ANN with two hidden layers. Acc\_Orig means the accuracy tested on original samples. Acc\_OT means the accuracy tested with one time inference. Acc\_LAP means the accuracy tested with the Largest Average Probabilities criterion.

Activations + Entropy	Acc_Orig	Acc_OT	Acc_LAP
Sigmoid (trained by BP)	0.99	0.62	
Sigmoid	0.98	0.83	0.84
Threshold	0.95	0.81	0.83
$y =  x $	0.96	0.83	0.84
$y = \arctan(1/x)$	0.98	0.82	0.84
$y = \ln -x $	0.97	0.81	0.83
Activations + 0-1 loss	Acc_Orig	Acc_OT	Acc_LAP
Sigmoid	0.87	0.78	0.79
Threshold	0.86	0.77	0.79
$y = \ln -x $	0.88	0.78	0.79

Table 2. Adversarial tests for ANNs with different activation and loss functions trained by GLR. The adversarial samples are generated by an ANN with five hidden layers. Acc\_Orig means the accuracy tested on original samples. Acc\_OT means the accuracy tested with the one time inference. Acc\_LAP means the accuracy tested with the Largest Average Probabilities criterion.

In Tables.1 and 2, an ANN with one hidden layer trained by the BP method reaches an accuracy of 0.99 in predicting the original samples. However, we can see in Tables.1 and 2, the accuracy of the same ANN reduces dramatically to 0.28 and 0.62 in predicting the adversarial samples generated by an ANN with two hidden layers and five hidden layers, respectively. This substantiates an observation in literature, i.e., the adversarial samples can effectively attack the ANN under a different architecture. It has been well-known that the output loss of an ANN typically has many local optima and saddle points. A conjecture on why this adversarial phenomenon happens is that the parameters in the ANN trained by the BP method may be stuck in a local optimum of the output loss with a very steep slope around the neighborhood or a saddle point. Therefore, a slight perturbation in the input data could lead to a significant changes in the outputs, which in turn causes the dramatic change in classification.

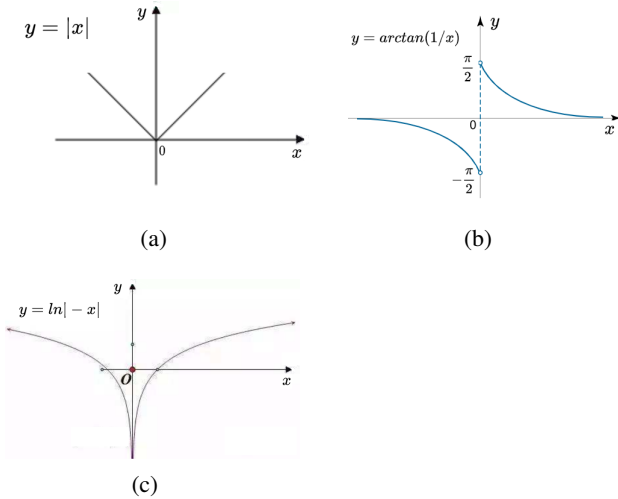


Figure 7. Three activation functions: (a)  $y = |x|$ ; (b)  $y = \arctan(1/x)$ ; (c)  $y = \ln|x| - x$ .

All ANNs with the entropy loss function trained by the GLR method achieve accuracies in predicting original samples comparable to the ANN trained by the BP method (above 95% in accuracy). Notice that GLR can train the ANNs with discontinuous activation functions, e.g., threshold function and  $y = \arctan(1/x)$ , and discontinuous loss functions, e.g. 0-1 loss, which cannot be handled by BP. Moreover, the ANNs trained by the GLR method have much higher accuracies (about 20% increase) in predicting adversarial samples compare to the ANN trained by the BP method. In Table.2, we can see accuracies of the ANNs trained by the new method reach above 80% without using any information of adversarial directions in training, a significant achievement relative to the existing results in the literature of addressing the adversarial attacks. In Table.1, another interesting observation is that although the ANNs with 0-1 loss reach accuracies less than 90% in predicting original samples, they lead to even higher accuracies in predicting the adversarial samples than the ANNs with cross entropy loss. In addition, we can see LAP has a slight edge over OT in the experiments.

The ANNs trained by the GLR method contain neuronal noises, and GLR does not differentiate the loss and activation functions so that it would not lead to the vanishing gradient issue (Pascanu et al., 2013). Therefore, the parameters in the ANNs trained by GLR is likely to avoid being stuck in some unstable local optima and saddle points, while they tend to converge to the stationary points with relatively flat slopes around their neighborhoods, which are more robust against the changes in the input data. This conjecture may explain why the ANNs trained by the GLR method can significantly improve the defensiveness against the adversarial attacks.

## 4. Conclusions

In this work, a GLR method is proposed for training ANNs with neuronal noises. Unlike the classic BP method, the GLR trains ANNs directly by the loss value rather than the gradient of loss and can handle ANNs with discontinuous activation and loss functions because it does not differentiate the loss output. Therefore, the GLR method could be a powerful tool to explore some brain-like learning mechanisms which allow more freedom to better represent the surrounding environment. The GLR method significantly improves defensiveness of the ANNs against adversarial attacks without using the adversarial direction in training, which indicates that the new training method is a very promising tool for enhancing the security of ANNs used in practice.

A future direction lies in reducing the variance of the stochastic gradient estimation for ANNs and speed up the training procedure, so that our method can be used in the deep learning ANNs with higher complexity. Adding regularization functions to the loss function for further improving adversarial defensiveness also deserves future research.

## References

- Alhussein Fawzi, S.-M. M.-D. and Frossard, P. Robustness of classifiers: from adversarial to random noise. *In Advances in Neural Information Processing Systems*, pp. 1632-1640, 2016.
- Asmussen, S. and Glynn, P. W. *Stochastic Simulation: Algorithms and Analysis*, volume 57. Springer Science & Business Media, 2007.
- C. Szegedy, W. Zaremba, I. S. J. B. D. E. I. G. and Fergus, R. Intriguing properties of neural networks. *In International Conference on Learning Representations*, 2014.
- Cao, X. and Gong, N. Mitigating evasion attacks to deep neural networks via region-based classification. *In Proceedings of the 33rd Annual Computer Security Applications Conference*, 278-287, 2017.
- Carlini, N. and Wagner, D. Towards evaluating the robustness of neural networks. *In Security and Privacy (SP), 2017 IEEE Symposium on*, pp. 3957, 2017.
- Carlini, N., Mishra, P., Vaidya, T., Zhang, Y., Sherr, M., Shields, C., Wagner, D., and Zhou, W. Hidden voice commands. *In USENIX Security Symposium*, 513-530, 2016.
- Dayan, P. and Abbott, L. *Theoretical Neuroscience*. The MIT Press, 2018.
- Elsayed, G. F., Shankar, S., Cheung, B., Papernot, N., Kurakin, A., Goodfellow, I. J., and Sohl-Dickstein, J. Ad-



- 
- versarial examples that fool both human and computer vision. *CoRR*, abs/1802.08195, 2018.
- Esteva, A., Kuprel, B., Novoa, R. A., Ko, J., Swetter, S. M., Blau, H. M., and Thrun, S. Dermatologist-level classification of skin cancer with deep neural networks. *Nature*, 542:115–, 2017.
- Eykholt, K., Evtimov, I., Fernandes, E., Li, B., Rahmati, A., Xiao, C., Prakash, A., Kohno, T., and Song, D. Robust Physical-World Attacks on Deep Learning Visual Classification. 2018.
- Fu, M. C. Stochastic gradient estimation. In *Fu, Michael C. (ed.), Chapter 5 in Handbooks of Simulation Optimization*, pp. 105–147. Springer, 2015.
- Glasserman, P. *Gradient Estimation via Perturbation Analysis*. Kluwer Academic Publishers, Boston, 1991.
- Goodfellow, I., Shlens, J., and Szegedy, C. Explaining and harnessing adversarial examples. *arXiv*, preprint arXiv:1412.6572, 2014.
- Graves, A., Mohamed, A., and Hinton, G. Speech recognition with deep recurrent neural networks. In *2013 IEEE International Conference on Acoustics, Speech and Signal Processing*, pp. 6645–6649, 2013.
- Gu, S. and Rigazio, L. Towards deep neural network architectures robust to adversarial examples. *CoRR*, abs/1412.5068, 2014.
- Gulshan, V., Peng, L., Coram, M., Stumpe, M. C., Wu, D., Narayanaswamy, A., Venugopalan, S., Widner, K., Madams, T., Cuadros, J., Kim, R., Raman, R., Nelson, P. Q., Mega, J., and Webster, D. Development and validation of a deep learning algorithm for detection of diabetic retinopathy in retinal fundus photographs. *JAMA*, 2016.
- Haykin, S. S. *Neural Networks and Learning Machines*, volume 3. Pearson Upper Saddle River, NJ, USA:, 2009.
- He, K., Zhang, X., Ren, S., and Sun, J. Deep residual learning for image recognition. In *Conference on Computer Vision and Pattern Recognition*, pp. 770–778, 2016.
- Heidergott, B. and Leahu, H. Weak differentiability of product measures. *Mathematics of Operations Research*, 35(1):27–51, 2010.
- Ho, Y.-C. and Cao, X.-R. *Discrete Event Dynamic Systems and Perturbation Analysis*. Kluwer Academic Publishers, Boston, MA, 1991.
- Hong, L. J. Estimating quantile sensitivities. *Operations Research*, 57(1):118–130, 2009.
- Kushner, H. J. and Yin, G. G. *Stochastic Approximation and Recursive Algorithms and Applications*. Springer, 2003.
- Liao, F., Liang, M., Dong, Y., Pang, T., Zhu, J., and Hu, X. Defense against adversarial attacks using high-level representation guided denoiser. *CoRR*, abs/1712.02976, 2017.
- N. Papernot, P. McDaniel, S. J. M. F. Z. B. C. and Swami, A. The limitations of deep learning in adversarial settings. In *Security and Privacy, 2016 IEEE European Symposium on*, pp. 372387, 2016.
- Osbert Bastani, Yani Ioannou, L. L. D. V. A. N. and Criminisi, A. Measuring neural net robustness with constraints. In *Advances in Neural Information Processing Systems*, pp. 26132621, 2016.
- Pascanu, R., Mikolov, T., and Bengio, Y. On the difficulty of training recurrent neural networks. In *International Conference on Machine Learning*, pp. 1310–1318, 2013.
- Peng, Y., Fu, M. C., Hu, J.-Q., and Heidergott, B. A new unbiased stochastic derivative estimator for discontinuous sample performances with structural parameters. *Operations Research*, 66(2):487–499, 2018.
- Peng, Y., Xiao, L., Heidergott, B., Hong, L. J., and Lam, H. Stochastic gradient estimation for artificial neural network. 2019.
- Pflug, G. C. *Optimization of Stochastic Models*. Kluwer Academic, Boston, 1996.
- Rubinstein, R. Y. and Shapiro, A. *Discrete Event Systems: Sensitivity Analysis and Stochastic Optimization by the Score Function Method*. Wiley, New York, 1993.
- S. Sabour, Y. Cao, F. F. and Fleet, D. J. Adversarial manipulation of deep representations. *arXiv*, preprint arXiv:1511.05122, 2015.
- Seyed-Mohsen Moosavi-Dezfooli, A. F. and Frossard, P. Deepfool: a simple and accurate method to fool deep neural networks. In *Proceedings of the IEEE Conference on Computer Vision and Pattern Recognition*, pp. 25742582, 2016.
- Silver, D., Huang, A., Maddison, C. J., Guez, A., Sifre, L., Driessche, G. V. D., Schrittwieser, J., Antonoglou, I., Panneershelvam, V., and Lanctot, M. Mastering the game of go with deep neural networks and tree search. *Nature*, 529(7587):484–489, 2016.